ELSEVIER

Polymer 44 (2003) 711–717

polymer

www.elsevier.com/locate/polymer

Crystallization and structure formation of poly(L-lactide-*co*-*meso*-lactide) random copolymers: a time-resolved wide- and small-angle X-ray scattering study

Jaedong Cho[a], Stephen Baratian[a,1], Jangsoon Kim[a], Fengji Yeh[b], Benjamin S. Hsiao[b], James Runt[a,*]

[a]*Department of Materials Science and Engineering and Materials Research Institute, The Pennsylvania State University, University Park, PA 16802, USA*
[b]*Department of Chemistry, State University of New York, Stony Brook, NY 11794, USA*

Received 24 October 2002; accepted 29 October 2002

Abstract

Time-resolved synchrotron simultaneous wide-angle X-ray diffraction (WAXD) and small-angle X-ray scattering (SAXS) experiments were used to investigate the crystallization behavior and microstructure development of poly(L-lactide), PLLA, and two random copolymers containing L-lactide (predominately) and randomly placed *R* stereochemical defects. The general features of crystallization of PLLA and the copolymers are similar except that the copolymers crystallize much more slowly and to a lesser extent than PLLA, as expected. Lamellar thicknesses derived from SAXS experiments are in very good agreement with mean thicknesses determined in a tapping mode AFM study of the same materials. The reduction in lamellar thickness and crystallinity with increasing *meso*-lactide content supports significant exclusion of the *R* stereoisomer from crystalline lamellae. In a separate series of time-resolved WAXD/SAXS experiments, each (co)polymer was crystallized for a fixed time, then heated to above its melting point. The observed behavior suggests a model for crystallization of the copolymers in which thinner lamellae form between 'primary' lamellar stacks during crystallization, with an average lamellar thickness that decreases with increasing *R* stereoisomer content.

Keywords: Crystallization; Polylactides; Random copolymers

1. Introduction

There has been significant academic and industrial interest in the polylactide family of materials. The lactide monomer can be derived from renewable agricultural sources, and relatively low cost monomer production has generated industrial interest in large volume production of fibers and films. In addition, polylactides are biocompatible and exhibit controllable hydrolysis/decomposition capability that yields nontoxic products [1]. Polylactide copolymers with polyglycolide have long been used as bioresorbable sutures. Polylactides are also under consideration in controlled drug release applications [2], porous scaffolds for tissue engineering [3,4] and other biomedical applications [5,6].

It is well known that the rate of hydrolytic degradation of polylactides and other aliphatic polyesters is strongly affected by the degree of crystallinity [7,8]. Therefore, it is natural to expect that crystalline lamellar organization plays an important role in determining the decomposition rate [9]. Early studies on poly(L-lactide-*co*-*meso*-lactide) random copolymers demonstrated that the concentration of *meso*-lactide comonomer units strongly influenced the observed melting temperature (T_m) and crystallization rate [10,11]. In a recent series of crystallization and structural studies of poly(L-lactide-*co*-*meso*-lactide) [12,13] and poly(L-lactide-*co*-D-lactide) [14] random copolymers with high L-lactide content, relationships between comonomer concentration and crystallization rates, solid-state microstructure, and equilibrium melting temperatures (T_m^0) were further established. For both the *meso*- and D-lactide copolymers, overall crystallinity and spherulite growth rates are significantly reduced with increasing comonomer

* Corresponding author. Tel.: +1-814-863-2749; fax: +1-814-865-2917.
E-mail address: runt@matse.psu.edu (J. Runt).
[1] Present address: Kimberly-Clark, Roswell, GA 30076, USA.

0032-3861/03/$ - see front matter © 2002 Elsevier Science Ltd. All rights reserved.
PII: S0032-3861(02)00823-6

content, as is lamellar thickness. The reduction in lamellar thickness and crystallinity suggests significant comonomer exclusion from crystalline lamellae. Using a combination of optical microscopy and 'static' small angle X-ray scattering (SAXS) experiments, the morphology of the copolymers was found to be composed of spherulites or hedrites, containing significant pockets of non-crystalline chain segments between lamellar bundles (fibrils). For example, the fraction of the amorphous component residing between lamellar bundles for poly(L-lactide) was estimated to be ca. 50% at the crystallization temperatures investigated [14].

The present study is a continuation of research on polylactide random copolymers containing stereochemical defects. We focus in the present paper on bulk crystallization kinetics and lamellar microstructure development of poly(L-lactide) and two poly(L-lactide-*co*-*meso*-lactide) copolymers from the quiescent molten state. An experimental approach was employed that has been successfully used by the authors in the study of poly(glycolide/lactide) copolymers [9,15] and crystalline polymer blends [16,17]: time-resolved, simultaneous wide-angle X-ray diffraction (WAXD) and small-angle X-ray scattering (SAXS) experiments. The current paper represents the first report of real time scattering experiments on poly(L-lactide) and its copolymers containing stereochemical defects.

2. Experimental

2.1. Materials

The polymers used in our experiments were synthesized from one or more cyclic lactides. A given dimeric lactide is composed of two lactic acid units and possesses two chiral carbon atoms. Two stereochemical isomers are possible: the *S* and *R* configurations. When polymerized, L-lactide results in placement of two *S* isomers in the chain, while *meso*-lactide results in the introduction of one *R* and one *S* unit.

Three polymers were investigated in the present study: poly(L-lactide) (PLLA) and two L-lactide/*meso*-lactide copolymers, containing 3 and 6% *meso*-lactide in the polymerization feed. The polymers were synthesized as described in Ref. [12]. NMR analysis has demonstrated that comonomer placement in similar copolymers is essentially random [18]. In other words, unpaired *R* stereodefects are placed randomly in chains containing predominately the *S* stereoisomer. Polystyrene-equivalent molecular weights are listed in Table 1 along with equilibrium melting points (T_m^0) estimated in one of our earlier studies [12]. *R* stereoisomer content was determined using chiral liquid chromatography and is also listed in Table 1. *R* concentrations deviated slightly from the predicted values based on the dimer feed ratio, presumably as a consequence of racemization of a small amount of *S* stereoisomer during polymerization [19]. Finally, the calculated number average sequence length of *S* isomers is also included in Table 1 [14].

2.2. Sample preparation

The polymer powders were dried at 80 °C under vacuum for 48 h. The powders were then compression molded into sheets by placing them in a Carver hydraulic press at 10,000 psi for 3 min, 30 °C above T_m^0. The sheets were removed from the press and cooled in air. Samples for the time-resolved WAXD/SAXS experiments were prepared by cutting ~7 mm diameter discs from the sheets and stacking them inside a ~1.5 mm thick copper sample holder. The discs were then brought to the nominal melting point (T_m) and allowed to fuse together in the holder. A small amount of pressure was applied to the top surface of the polymer with a metal cylinder to assist in consolidating each sample. The samples were cooled to room temperature and Kapton films were placed over the surfaces of the specimens.

2.3. Time-resolved WAXD/SAXS

Time-resolved simultaneous WAXD/SAXS experiments were conducted on the Advanced Polymers Beamline, X27C, at the National Synchrotron Light Source, Brookhaven National Laboratory. The X-ray wavelength was 0.1366 nm and pinhole collimation was utilized. Two linear position-sensitive detectors connected in series were used to collect the SAXS and WAXD data simultaneously. For SAXS, the sample to detector distance was 1.935 m, covering an angular range from $q = 0.06$ to 2.8 nm^{-1}, ($q = (4\pi/\lambda)\sin(\theta/2)$, where q is the scattering vector, θ the scattering angle and λ the wavelength). The WAXD 2θ range was ~5–35°, relative to $\lambda = 0.154$ nm. The scattering from silver behenate and aluminum oxide standards were used to calibrate the SAXS and WAXD detectors, respectively. Details of the beamline set-up have been described elsewhere [20].

The SAXS data were first smoothed using a moving window averaging procedure, and then background scattering due to thermal density fluctuations was subtracted [21]. The one-dimensional correlation function ($\gamma(r)$) was calculated from the scattering profile using the following

Table 1
Characteristics of poly(L-lactide-*co*-*meso*-lactide) copolymers

Copolymer	*R* content (%)	M_n	M_w	T_m^0, (°C) [12]	Average *S* run length
poly(L-lactide)	0.4	65,500	127,400	211–214	–
3% *meso*-lactide copolymer	2.1	65,800	122,600	200	54
6% *meso*-lactide copolymer	3.4	63,900	119,100	187	31

equation [22]

$$\gamma(r) = \int_0^\infty q^2 I(q)\cos(qr)\mathrm{d}q \quad (1)$$

where r is the distance and $I(q)$ is the intensity at a given q. The relative invariant (Q) was obtained as the ordinate of the linear fit to the self-correlation portion of the correlation function. For an ideal two-phase system with well-defined interfaces, the invariant per unit scattering volume is related to the difference between the electron densities of the crystalline and amorphous regions by

$$Q = Kv_s x_c(1 - x_c)\Delta\eta^2 \quad (2)$$

where K is a constant depending on the experimental conditions, x_c the linear crystallinity (given by the ratio of the mean lamellar thickness, l_c, to the long period, L), v_s the volume fraction of lamellar stacks (given by the ratio of the bulk crystallinity to the linear crystallinity) and $\Delta\eta$ the linear electron density difference defined as $\Delta\eta = \eta_c - \eta_a$, where η_c and η_a are the electron densities of the crystal and amorphous layers, respectively.

If B is the value of the abscissa where the ordinate first equals zero in $\gamma(r)$, and the long period is obtained from the first maximum of $\gamma(r)$, then $x_c(1 - x_c) = B/L$. When $x_c > 0.5$, the mean l_c in lamellar stacks can be determined from $l_c = x_c L$. Similarly, the average amorphous layer thickness within stacks (l_a) can be obtained from $l_a = (1 - x_c)L$. For $x_c < 0.5$, x_c is replaced by $(1 - x_c)$ in the above expressions. Further discussion of determination of l_c and l_a will be deferred to Section 3.

The real-time WAXD/SAXS experiments were conducted using a sample holder designed to allow for a rapid jump between the melting temperature and selected T_cs. A T_c of 123 °C was used for all three polymers, which is close to the temperature of maximum spherulite growth rate for each [12]. T_cs of 147 °C for PLLA and 136 °C for the 3% *meso* copolymer were also selected in order to evaluate crystallization behavior at a comparable degree of supercooling, ΔT ($= T_m^0 - T_c$). All samples were maintained for 5 min in the high temperature chamber ($> T_m^0$) prior to transferring to the crystallization chamber. In separate series of experiments, PLLA and the copolymers were isothermally crystallized for 40 min at 123 °C, then the temperature was ramped at a rate of 3 °C/min from T_c to a temperature $> T_m$.

Finally, degrees of crystallinity were determined from the WAXD data using a curve-fitting program. Diffraction profiles were separated into crystalline reflections and an amorphous background, all assuming Gaussian profiles. The apparent degree of crystallinity was defined as the ratio of the area under the resolved crystalline peaks to the total area. The experimental uncertainty in the measured crystallinities was on the order of several percent. When locations of WAXD diffractions peaks are discussed in Section 3, the values have been referenced to $\lambda = 0.1542$ nm (i.e. Cu Kα).

3. Results and discussion

The development of WAXD and SAXS profiles during crystallization of PLLA at 123 °C is displayed in Fig. 1. The wide-angle diffraction peaks observed for PLLA and the copolymers are those expected for the usual α-form of PLLA (orthorhombic unit cell) [23,24]. Several diffraction peaks are seen in Fig. 1a, with the most prominent being a very strong reflection at $2\theta = 16.7°$ (due to diffraction from (200) and/or (110) planes) and a strong reflection at $2\theta = 19.1°$ (arising from (203)). In addition, two weak reflections are observed at $2\theta = 12.5$ and $22.4°$ (due to diffraction from (103) and (015) planes, respectively) and a moderate-intensity peak at $2\theta = 14.8°$ (arising from (010)). No systematic changes in diffraction peak positions or peak widths at half height were detected during isothermal crystallization of any of the samples.

Relatively sharp maxima near $q \sim 0.035$ Å^{-1} are observed in the Lorentz-corrected SAXS profiles displayed in Fig. 1b. A weak second order maximum is also seen in Fig. 1b near the end of isothermal crystallization. The intensity of this second order reflection decreased significantly for the 3% *meso*-lactide copolymer and essentially disappeared for the 6% *meso*-lactide copolymer crystallized at the same T_c, indicating less well-defined lamellar stacks with increasing comonomer content (even though ΔT decreases for the copolymers compared to PLLA). The final long period increases by a small amount with

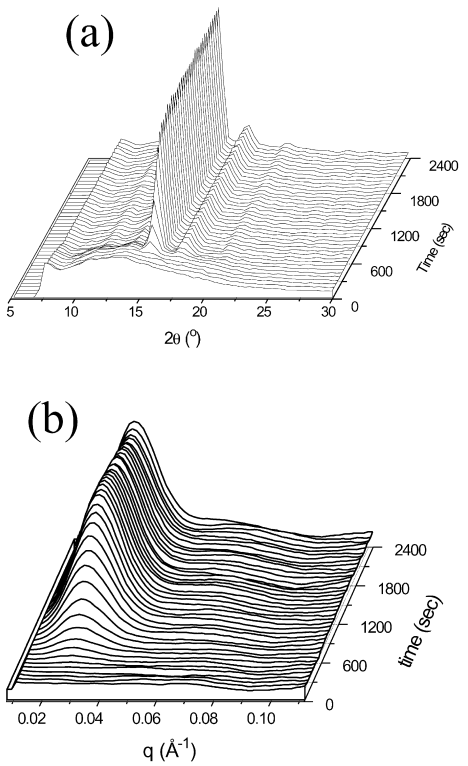

Fig. 1. (a) Development of WAXD and (b) Lorentz-corrected SAXS profiles as a function of crystallization time for PLLA at $T_c = 123$ °C. 2θ is relative to $\lambda = 0.154$ nm.

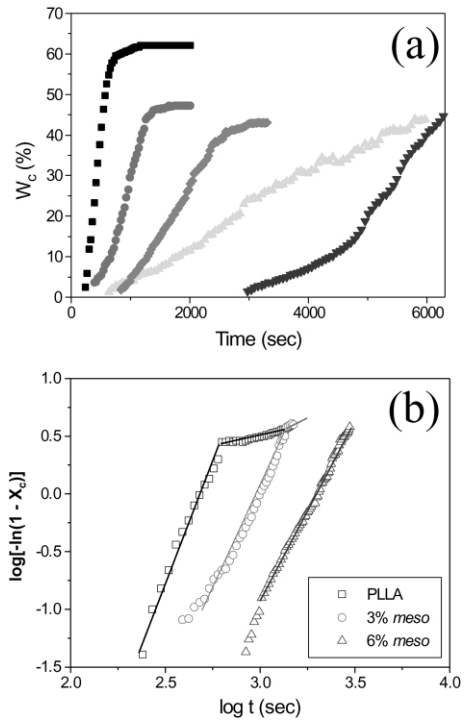

Fig. 2. (a) Development of WAXD crystallinity as a function of comonomer concentration and crystallization temperature. ■, PLLA at $T_c = 123$ °C; ▼, PLLA at $T_c = 147$ °C; ●, 3% *meso* copolymer at $T_c = 123$ °C; ▲, 3% *meso* copolymer at $T_c = 136$ °C; ◆, 6% *meso* copolymer at $T_c = 123$ °C; (b) Avrami plots of copolymers at $T_c = 123$ °C; for the data displayed in part (a).

increasing *meso*-lactide content at $T_c = 123°$ C. These values are larger for PLLA crystallized at 147 °C and the 3% *meso*-lactide copolymer crystallized at 136 °C.

Although not immediately evident in Fig. 1, the SAXS invariant consistently develops prior to the appearance of WAXD crystallinity for all specimens, a common observation during crystallization in time-resolved simultaneous WAXD/SAXS experiments. The origin of this remains controversial, however, it has been associated with spinodal decomposition [25], relative detector sensitivities [26], and primary nucleation [27]. For all samples, the development of the SAXS invariant mirrors that of the time dependent WAXD crystallinity: both increase in a more or less sigmoidal fashion during the course of crystallization, as depicted in Figs. 2 and 3. The general features of crystallization of PLLA and the *meso*-lactide copolymers are very similar except that the copolymers crystallize much more slowly than PLLA (see crystallization half-times, $t_{1/2}$, in Table 2) [11,12]. Bulk crystallinities at the end of isothermal crystallization ($W_{c,final}$) decrease with increasing *R* stereoisomer content, as seen in Fig. 2a and Table 2. The crystallinity data are presented in classic double log Avrami form for the three samples crystallized at 123 °C in Fig. 2b. The Avrami equation can be written as: [28]

$$1 - X_c = \exp(-zt^n) \quad (3)$$

where X_c is the fraction of the final crystallinity developed

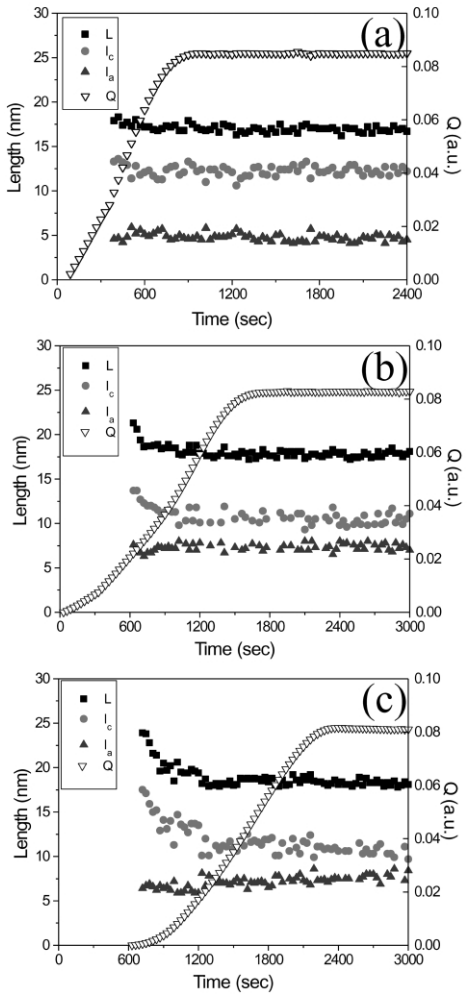

Fig. 3. Crystallization time dependence of the mean long period, lamellar thickness and amorphous layer thickness in lamellar stacks, along with the SAXS invariant for (a) PLLA (b) the 3% *meso*-lactide copolymer, and (c) the 6% *meso* copolymer, crystallized at 123 °C.

up to time *t*, *z* is a function of the nucleation and growth rates, and *n* is related to the growth geometry and type of nucleation. The data for PLLA at $T_c = 123°$ C clearly must be fit by two values of *z* and *n* (Table 2). The dominant process for all three polymers at $T_c = 123$ °C is best fit with $n \sim 3$–4, typical of spherulitic growth. For PLLA and the

Table 2
Avrami parameters derived from time-resolved WAXD

Sample (T_c)	$t_{1/2}$ (s)	$W_{c,final}$ (%)	$X_{c,s}$[a] (%)	*n*	*z*
PLLA (123 °C)	430	62	94	4.0	1.7×10^{-11}
				0.4	1.9×10^{-1}
PLLA (147 °C)	5220	48		5.4	6.7×10^{-21}
3% *meso*-lactide (123 °C)	915	47	98	3.8	5.2×10^{-12}
				0.7	3.1×10^{-2}
3% *meso*-lactide (136 °C)	2900	44		1.9	1.5×10^{-7}
6% *meso*-lactide (123 °C)	1780	43		3.3	1.3×10^{-11}

[a] Relative crystallinity at the end of the first process.

3% *meso*-lactide copolymer, this is followed by a secondary process with $n \sim 0.4-0.7$ (similar to values reported during secondary crystallization of other polymers [29,30]), although the longer time process does not become apparent until later in the crystallization of the 3% copolymer. This behavior was confirmed in a separate DSC crystallization study of the same (co)polymers [31]. A second crystallization stage was not detected for the slowly crystallizing 6% copolymer, similar to our previous observations on slowly crystallizing polymer blends [17]. The Avrami plots for PLLA crystallized at 147 °C and the 3% *meso*-lactide copolymer crystallized at 136 °C were also best single fit by single values of n and z, and the n values are well outside the range determined for the samples at $T_c = 123$ °C. An Avrami exponent of ~2 for the 3% copolymer crystallized at 136 °C is particularly surprising since both optical microscopy and atomic force microscopy experiments show a spherulitic/hedritic growth morphology at this crystallization temperature. It is unclear at this point whether secondary crystallization would be observable for the more slowly samples if experiments were carried out for much longer times, or whether this behavior indicates that of the nature of the crystallization process has changed for higher comonomer content materials (and at lower ΔT).

Before moving on to the results of the simultaneous time-resolved SAXS experiments, it is important to note how l_c and l_a are determined from $\gamma(r)$. As mentioned earlier, l_c and l_a can in principle be derived from the correlation function, but secondary evidence must be used to clearly distinguish between them. The criteria we used were as follows. From the definition of the linear crystallinity, $x_c \geq \phi_c$, where ϕ_c is the volume fraction crystallinity. Secondly, l_c is well known to increase with increasing T_c. Most importantly, we recently conducted a tapping mode atomic force microscopy (AFM) study on the identical (co)polymers crystallized at temperatures similar to those employed here [32]. Mean lamellar thicknesses were determined by direct visualization of edge-on lamellae from AFM height and phase images after crystallization at a variety of temperatures. The AFM data provide independent verification of the l_c values and X-ray scattering model ('finite' lamellar stacks).

The mean long period and lamellar thickness are frequently observed to decrease in the early stages of polymer crystallization in time-resolved SAXS experiments [9,15–17] and the behavior of the polylactides under investigation here are no exception. The crystallization time dependence of the SAXS invariant and microstructural parameters for PLLA at 123 °C is shown in Fig. 3a. Early in the crystallization process, L and l_c decrease by ~1 nm (l_a is constant), then become time independent. The initial decrease in L and l_c is significantly larger for the copolymers: ~3 nm for 3% *meso* copolymer and ~6 nm for the 6% copolymer (Fig. 3b and c, respectively). Like PLLA and the 3% *meso*-lactide copolymer, the long period for the 6% *meso* copolymer (Fig. 3c), remains constant with time after the initial decrease. However, l_c for the 6% *meso* copolymer continues to decrease throughout crystallization, accompanied by a gradual increase in l_a of ~2 nm. Similar behavior is observed for the slowly crystallizing PLLA at 147 °C and 3% *meso*-lactide copolymer at 136 °C (not shown). Such behavior has frequently been explained by crystallization of thinner, perhaps more defective lamellar stacks between existing primary stacks consisting of lamella with larger thickness [9,15]. Alternatively, on the basis of real-time AFM experiments during poly(ethylene terephthalate) crystallization as well as some modeling, other authors have argued that an increasing number of lamella per stack is responsible for the reduction in L at short crystallization times [33]. However, the latter is not consistent with the results of the simultaneous WAXD/SAXS experiments during melting of the polylactide (co)polymers, as will be discussed shortly.

Lamellar structural parameters at the conclusion of the time-resolved experiments are summarized in Table 3. It is important to note that the final lamellar thickness for PLLA at $T_c = 123$ °C is identical within experimental uncertainty with the value determined from tapping mode AFM experiments [32]. In addition, the AFM measurements lead us to assign the larger length to l_c for the 6% *meso*-lactide copolymer, in contrast to the assignment in our earlier paper [12]. For PLLA crystallized at 147 °C, the final $l_c \sim 15$ nm, about 3 nm larger than at 123 °C. The mean lamellar thickness at the highest T_c explored in the AFM experiments (141 °C) was 16.5 nm, comparable to that determined from SAXS at the end of the crystallization experiment at 147 °C. Lamellar thickness decreases somewhat with increasing comonomer content at the same T_c, even though the copolymers are crystallized at a smaller ΔT at 123 °C. At comparable ΔT, l_c decreases significantly with comonomer content (from ~15 to 10 nm). These results emphasize the importance of defect comonomer content in establishing lamellar structure in these and other random copolymers, where the *co*-units are largely rejected from the crystalline phase. Lastly, the final linear crystallinity decreases for the copolymers compared to PLLA, indicating greater incorporation of amorphous segments in lamellar stacks [12].

In a separate series of time-resolved X-ray scattering experiments, each (co)polymer was crystallized at 123 °C for 40 min and then heated to 200 °C.[2] A summary of the time (and temperature) dependent microstructure parameters and bulk crystallinity for PLLA and the *meso*-lactide copolymers are displayed in Figs. 4a–c. The apparent melting point (defined here as the disappearance of crystallinity) decreases with increasing *meso*-lactide content: from 165 to 162 to 153 °C. As temperature is increased after crystallization, PLLA crystallinity gradually decreases

[2] The apparent temperatures of the polylactide samples depicted in Fig. 4 are higher than those experienced by the interior of the specimens, as a consequence of thermal lag associated with the relatively large specimen size required in the temperature jump experiments [16].

Table 3
Final microstructural parameters for the polylactides from SAXS

Sample (T_c)	L (nm)	l_c (nm)	l_a (nm)
PLLA (123 °C)	16.9	12.3	4.6
PLLA (147 °C)	21.9	15.1	6.8
3% *meso*-lactide (123 °C)	18.0	10.7	7.3
3% *meso*-lactide (136 °C)	19.2	11.6	7.6
6% *meso*-lactide (123 °C)	18.1	10.3	7.8

while the mean L, l_c and l_a increase significantly until the specimen is completely molten (Fig. 4a). The increase in lamellar and amorphous layer thickness on heating is 7–8 nm. Such behavior is not in keeping with a mechanism of 'simple' lamellar thickening or a decreasing number of lamella per stack during heating. However, the data are consistent with crystallization of thinner lamella within or between lamellar stacks during crystallization. Thinner lamella would be the first to melt on subsequent heating, leading to an increase in measured L, l_c and l_a in general agreement with the observations in Fig. 4a. Crystal thickening via partial melting and recrystallization cannot be completely ruled out, but lamellar thickening during melting was not found to be significant in an earlier DSC study of PLLA and the *meso*-lactide copolymers, crystallized at temperatures comparable to those employed here [12].[3]

For the 3% *meso*-lactide copolymer (Fig. 4b), the microstructural parameters also increase significantly as T_m is approached. The increase in lamellar thickness is comparable to PLLA, but the increase in l_a on heating is somewhat smaller (~6 nm). This trend continues for the 6% *meso*-lactide copolymer (Fig. 4c): again, the increase in l_c on heating is comparable to PLLA but the amorphous layer thickness in lamellar stacks increases by only ~2–3 nm as T_m is approached. This behavior suggests a model for crystallization of the copolymers in which progressively thinner lamella form between 'primary' lamellar stacks with increasing *meso*-lactide content. On heating to T_m, the mean lamellar thickness increases significantly due to the melting of the thinner lamella but the average l_a is affected to a lesser extent as *meso*-lactide content increases.

4. Summary

We report on the simultaneous investigation of crystallization kinetics and microstructure development from the quiescent melt of PLLA and two poly(L-lactide-*co*-*meso*-lactide) copolymers using time-resolved WAXD/SAXS. Development of the SAXS invariant and time dependent WAXD crystallinity mirror each other, with both increasing

[3] As defect concentration increases, it is unlikely that widespread lamellar thickening would occur on heating random copolymers in which the chain defects are largely rejected from the crystals under typical crystallization conditions.

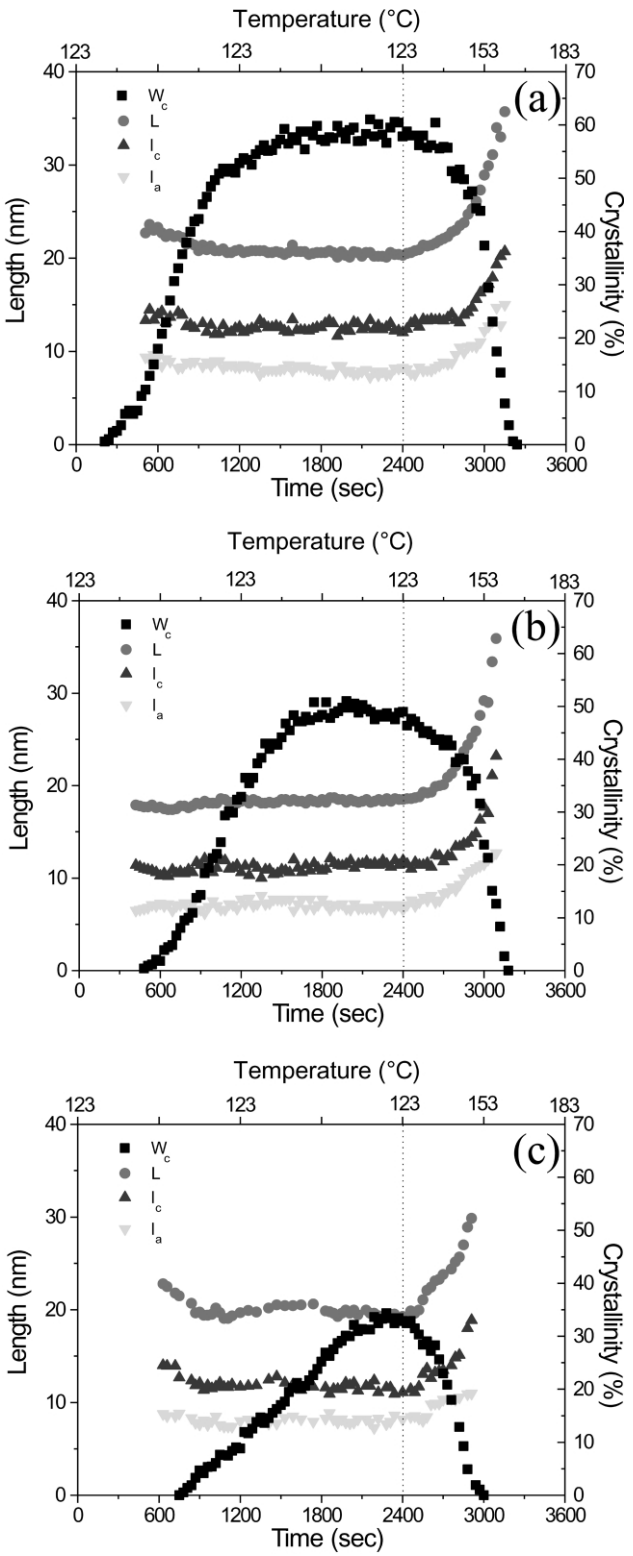

Fig. 4. Microstructural parameters and WAXD crystallinities as a function of time during crystallization of (a) PLLA (b) the 3% *meso*-lactide copolymer and (c) the 6% *meso* copolymer at $T_c = 123$ °C; and then melting at 3 °C/min after isothermal crystallization. ■, WAXD crystallinity; ●, long period; ▲, lamellar thickness; ▼, amorphous layer thickness. The vertical dashed lines indicate the onset of heating.

in a sigmoidal fashion during the course of primary crystallization. The general features of crystallization of PLLA and the *meso*-lactide copolymers are similar, although the copolymers crystallize more slowly and to a lesser extent than PLLA. For PLLA and the 3% *meso*-lactide copolymer, the dominant crystallization process (characterized by an Avrami exponent in the range of 3–4) is followed by a second process with $n \sim 0.5$, similar to the value reported during secondary crystallization of other polymers [29,30].

At comparable ΔT, l_c decreases significantly with comonomer content (from ~15 to 10 nm). These results illustrate the importance of comonomer content in establishing lamellar structure in these and other random copolymers, where *co*-units are principally rejected from the crystalline phase. Microstructural parameters (L, l_c and l_a) increase significantly on heating PLLA from T_c to T_m. Similar behavior is observed for the 3% and 6% *meso*-lactide copolymers, but the increase in l_a on heating is smaller than that observed for PLLA—and less so at higher *R* content. This behavior suggests a copolymer crystallization model in which thinner lamella crystallize between dominant lamellar stacks, with a lamellar thickness that decreases with increasing *R* stereoisomer content.

Acknowledgements

The Penn State authors would like to express their appreciation to the National Science Foundation (DMR-9900638) and the donors of the ACS Petroleum Research Fund for support of this research. BSH and FY thank a US Department of Energy grant (DEFG0299ER45760) for support of the AP-PRT beamline. We would also like to thank Eric S. Hall of Cargill Dow Polymers for synthesizing the polymers used in this study.

References

[1] Vert M, Schwarch G, Coudane J. J Macromol Sci Pure Appl Chem 1995;A32:787.
[2] Fu YJ, Mi FL, Wong TB, Shyu SS. J Microencapsulat 2001;18:733.
[3] Langer R, Vacanti JP. Science 1993;260:920.
[4] Lu LC, Zhu X, Valenzuela RG, Currier BL, Yaszemski MJ. Clin Orthopaed Rel Res 2001;391:S251.
[5] Zhang X, Goosen MFA, Wyss UP, Pichora DJ. Macromol Sci Rev Macromol Chem Phys 1993;C33:81.
[6] Durselen L, Dauner M, Hierlemann H, Planck H, Claes LE, Ignatius A. J Biomed Mater Res 2001;58:666.
[7] Mochizuki M, Hirami M. Polym Adv Technol 1997;8:203.
[8] Tsuji H, Ikeda Y. J Appl Polym Sci 1997;63:855.
[9] Wang ZG, Hsiao BS, Zong XH, Yeh F, Zhou JJ, Dormier E, Jimiolkowski DD. Polymer 2000;41:621.
[10] Fischer EW, Sterzel HJ, Wegner G. Kolloid ZZ Polym 1973;251:980.
[11] Kolstad JL. J Appl Polym Sci 1996;62:1079.
[12] Huang J, Lisowski MS, Runt J, Hall ES, Kean RT, Buehler N, Lin JS. Macromolecules 1998;31:2593.
[13] Runt J, Huang J, Lisowski MS, Hall ES, Kean R, Lin JS. In: Scholtz C, Gross RA, editors. Polymers from renewable resources—biopolyesters and biocatalysis. ACS Symposium Series No. 764; 2000. Chapter 15.
[14] Baratian S, Hall ES, Lin JS, Xu R, Runt J. Macromolecules 2001;34:4857.
[15] Wang ZG, Wang X, Hsiao BS, Andjelic S, Jamiolkowski D, McDivitt J, Fischer J, Zhou J, Han CC. Polymer 2001;42:8965.
[16] Lisowski MS, Liu Q, Cho J, Runt J, Yeh F, Hsiao BS. Macromolecules 2000;33:4842.
[17] Cho J, Xu R, Yeh F, Hsiao BS, Runt J. Macromol Symp. Submitted for publication.
[18] Thakur KAM, Kean RT, Hall ES, Kolstad JJ, Lindgrenn TA, Doscotch MA, Siepmann JI, Munson EJ. Macromolecules 1997;30:2422.
[19] Kricheldorff HR, Dunsing R. Makromol Chem 1986;187:1611.
[20] Hsiao BS, Chu B, Yeh F. NSLS Newsletter 1997;(July):1.
[21] Hsiao BS, Verma RK. J Synchrontron Rad 1998;5:23.
[22] Strobl GR, Schneider M. J Polym Sci Polym Phys Ed 1980;18:1343.
[23] De Santis P, Kovacs A. Biopolymers 1968;6:299.
[24] Hergeth WD, Lebek W, Stettin E, Witkowski K, Schmutzler K. Makromol Chem 1992;193:1607.
[25] Olmsted PD, Poon WCK, McLeish TCB, Terrill NJ, Ryan AJ. Phys Rev Lett 1998;81:373.
[26] Wang ZG, Hsiao BS, Kopp C, Sirota EB, Srinivas S. Polymer 2000;41:8825.
[27] Chen EQ, Weng X, Zhang A, Mann I, Harris FW, Cheng SZD, Stein R, Hsiao BS, Yeh F. Macromol Rapid Commun 2001;22:611.
[28] Avrami MJ. Chem Phys 1939;7:1103.
[29] Akpalu Y, Kielhorn L, Hsiao BS, Stein RS, Russell TP, van Egmond J, Muthukumar M. Macromolecules 1999;32:705.
[30] Alizadeh A, Richardson L, Xu J, McCartney S, Marand H, Cheung YW, Chum S. Macromolecules 1999;32:6221.
[31] Xu R, Kanchanasopa M, Runt J. Unpublished results.
[32] Kanchanasopa M, Manias E, Runt J. Macromolecules. Submitted for publication.
[33] Ivanov DA, Amalou Z, Magonov SN. Macromolecules 2001;34:8944.